Biochimica et Biophysica Acta 1798 (2010) 579–591

Contents lists available at ScienceDirect

Biochimica et Biophysica Acta

journal homepage: www.elsevier.com/locate/bbamem

Role of membranotropic sequences from herpes simplex virus type I glycoproteins B and H in the fusion process

Stefania Galdiero [a,b,c], Annarita Falanga [a], Giuseppe Vitiello [d,e], Mariateresa Vitiello [f], Carlo Pedone [a,b,c], Gerardino D'Errico [d,e], Massimiliano Galdiero [b,f,*]

[a] Department of Biological Sciences, Division of Biostructures – University of Naples "Federico II", Via Mezzocannone 16, 80134, Napoli, Italy
[b] Centro Interuniversitario di Ricerca sui Peptidi Bioattivi – University of Naples "Federico II", Via Mezzocannone 16, 80134, Napoli, Italy
[c] Istituto di Biostrutture e Bioimmagini – CNR, Via Mezzocannone 16, 80134, Napoli, Italy
[d] Department of Chemistry, University of Naples "Federico II", CSGI – Monte Sant'Angelo, 80126, Napoli, Italy
[e] Consorzio per lo Studio dei Sistemi a Grande Interfase, CSGI – Monte Sant'Angelo, 80126, Napoli, Italy
[f] Department of Experimental Medicine – II University of Naples, Via De Crecchio 7, 80138, Napoli, Italy

ARTICLE INFO

Article history:
Received 14 September 2009
Received in revised form 11 January 2010
Accepted 12 January 2010
Available online 18 January 2010

Keywords:
Fusion peptide
Membrane
Virus
Surface plasmon resonance
Glycoprotein

ABSTRACT

The entry of enveloped viruses involves attachment followed by close apposition of the viral and plasma membranes. Then, either on the cell surface or in an endocytotic vesicle, the two membranes fuse by an energetically unfavourable process requiring the destabilisation of membrane microenvironment in order to release the viral nucleocapsid into the cytoplasm. The core fusion machinery, conserved throughout the herpesvirus family, involves glycoprotein B (gB) and the non-covalently associated complex of glycoproteins H and L (gH/gL). Both gB and gH possess several hydrophobic domains necessary for efficient induction of fusion, and synthetic peptides corresponding to these regions are able to associate to membranes and induce fusion of artificial liposomes. Here, we describe the first application of surface plasmon resonance (SPR) to the study of the interaction of viral membranotropic peptides with model membranes in order to enhance our molecular understanding of the mechanism of membrane fusion. SPR spectroscopy data are supported by tryptophan fluorescence, circular dichroism and electron spin resonance spectroscopy (ESR). We selected peptides from gB and gH and also analysed the behaviour of HIV gp41 fusion peptide and the cationic antimicrobial peptide melittin. The combined results of SPR and ESR showed a marked difference between the mode of action of the HSV peptides and the HIV fusion peptide compared to melittin, suggesting that viral-derived membrane interacting peptides all act via a similar mechanism, which is substantially different from that of the non-cell selective lytic peptide melittin.

1. Introduction

Peptide–lipid interactions play a central role in various biological processes, including the insertion and folding of membrane proteins, the formation of ion channels, translocation of polypeptides through membranes, the interaction of peptide hormones with membrane receptors, signal transduction, the action of antimicrobial and cytotoxic peptides, lipolysis and blood coagulation [1–3]. Subtle differences in the relative affinity of peptides for the phospholipids, as well as the orientation and degree of insertion of the peptide into the lipid bilayer, contribute to the biological function of these molecules and may also play a role in the recruitment and assembly of signalling complexes. The common structural feature of membrane-active peptides and proteins is the adoption of a stable secondary structure upon binding to the membrane surface.

Elucidation of the mechanism of membrane fusion for enveloped viruses has attracted considerable attention because of its relative simplicity and potential clinical importance [4,5]. The nature of the interaction of viral fusion proteins with membranes and the mechanism by which these proteins accomplish fusion are poorly understood.

The entry of enveloped viruses involves attachment followed by close apposition and fusion of the viral and plasma membranes. Then, either on the cell surface or in an endocytotic vesicle, the two membranes fuse by an energetically unfavourable process involving the destabilisation of membrane microenvironment in order to release the viral nucleocapsid into the cytoplasm. The fusion process requires a major conformational change of the viral fusion protein to expose a hydrophobic fusion peptide. This change can be induced by virus envelope glycoproteins binding to cellular receptors at neutral pH, and it occurs at the plasma membrane. Alternatively, the conformational change of the fusion protein is induced by an acidic

* Corresponding author. Department of Experimental Medicine – II University of Naples, Via De Crecchio 7, 80138, Napoli, Italy. Tel.: +39 081 5667646; fax: +39 081 5667578.
E-mail address: massimiliano.galdiero@unina2.it (M. Galdiero).

0005-2736/$ – see front matter © 2010 Elsevier B.V. All rights reserved.
doi:10.1016/j.bbamem.2010.01.006

pH. In this case, virus particles undergo endocytosis prior to the fusion.

Herpes simplex virus type I (HSV) enters cells by fusion of the viral and host-cell membranes; however, the mechanisms underlying the merging of these membranes are still unclear. Understanding the molecular basis of the fusion process is of critical importance for the design and development of therapeutic agents that could aid in the treatment of HSV-related illnesses.

The core fusion machinery, conserved throughout the herpesvirus family, involves glycoprotein B (gB) and the non-covalently associated complex of glycoproteins H and L (gH/gL) [6–8]. Although it is now clear that both gB and gH play a fusogenic role in herpesviruses, their precise mechanism of function is still unknown [7,8]. Based on the crystal structure, gB was proposed to be a fusion protein belonging to the new class III together with vesicular stomatitis virus (VSV) G protein and baculovirus gp64 [8,9]. However, gB does not function as a fusion protein in the absence of gH/gL [7]. In fact in a transfection model, only gH/gL is able to induce hemifusion while gB helps in accomplishing complete fusion [10]. The structure of gH is still unknown, but several indirect evidence suggest that this is a fusogenic protein as well. Recently, it has been reported that both gB and gH possess several hydrophobic domains necessary for efficient induction of fusion, and synthetic peptides corresponding to these regions are able to associate to membranes and induce fusion of artificial liposomes [11–15].

Moreover, there is converging evidence that protein domains other than the fusion peptide play an important and cooperative role in inducing fusion between a viral envelope and a cell membrane. This is particularly true for the complex fusion mechanism adopted by HSV where at least two proteins, gB and gH, act in concert to gain access into the cells.

Thus, it is likely that different protein domains cooperate in driving membrane fusion, but their membranotropic characteristics may differ, according to the role played by each single region.

The molecular details underlying the process of membrane fusion due to fusion peptides are only just starting to be understood and the role of numerous physicochemical parameters including peptide charge, hydrophobicity, amphipathicity and the degree of secondary structure and the angle subtended by the polar face, in the physicochemical interaction between viral peptides and the membrane are being analysed by several groups [1–3,8,16].

A wide variety of biophysical techniques have been used to study biomolecular–membrane interactions [17,18]. These techniques have provided important information on specific structure–function relationships associated with peptide–membrane interactions. To understand the role of membrane association in protein function it would be necessary to analyse the energetics of binding and insertion of peptides into the membrane, as well as to determine the correlation between the membrane induced conformational changes and the associated variation in the affinity to the membrane during binding. Hence, the complete characterization of the binding of fusion peptides to lipid surfaces also requires the definition of a mechanism of the interaction process and the determination of binding constants associated with each step of the proposed mechanism. Concerning this point, it is generally considered that the binding of membrane-active peptides to lipid membranes occurs via at least a two-step process [19,20]. Initially, the peptide binds electrostatically to the membrane localising itself near the surface, and then it could relocate on the surface or insert further into the hydrocarbon region of the lipid membrane by hydrophobic interactions. Since the binding reaction is very fast, it is quite difficult to distinguish the two binding steps and therefore it is a challenge to study this process using conventional techniques.

In recent years, Surface Plasmon Resonance (SPR) spectroscopy has become a widely used technique to study antibody–antigen, DNA–DNA, DNA–protein, protein–protein and receptor–ligand interactions [21–23] and also to quantitate these interactions through the measurement of kinetic rate constants and affinity constants. SPR spectroscopy has also been applied to the study of biomembrane-based systems [24,25]. A few studies were reported on the interaction of proteins or short peptides with phospholipid membranes. Most of them utilised hybrid lipid monolayers (using HPA sensor chip) [25,26], and only a few described the use of lipid bilayers (using the L1 sensor chip) [27], which more closely resemble biological membranes. Recently, Papo and Shai [28] have used monolayer and bilayer phospholipid membranes in SPR experiments to differentiate between pore-forming and non-pore-forming lytic peptides. Moreover, they showed that melittin formed pores only in zwitterionic membranes, whereas both melittin and the antimicrobial peptide magainin had a detergent-like effect on negatively charged membranes, similar to what has been predicted by others using different methods [29].

Here, we describe the first application of SPR to the study of the interaction of fusion peptides with model membranes in order to enhance our molecular understanding of the mechanism of viral-induced membrane fusion. The analysed peptides were selected from HSV-1 gB and gH and compared to the behaviour of HIV gp41 fusion peptide and the cationic antimicrobial peptide melittin. Moreover, our data are further supported by tryptophan fluorescence and electronic spin resonance spectroscopy. In particular, both the experiments were meant to gain deeper insight into the positioning of the peptides in lipid membranes, which is known to be crucial for their functionality [30–33].

2. Materials and methods

2.1. Materials

Fluorenylmethoxycarbonyl (Fmoc) protected amino acids were purchased from INBIOS (Pozzuoli, NA, Italy), NovaSyn TGA resin from Nova Biochem (Darmstadt, Germany). The reagents (piperidine, pyridine) for the solid-phase peptide synthesis were purchased from Fluka (Sigma-Aldrich, Milano, Italy), trifluoroacetic acid (TFA) and acetic anhydride were from Applied Biosystem (Foster City, CA, USA). H_2O, DMF and CH_3CN were supplied by LAB-SCAN (Dublin, Ireland). Dichloromethane and methanol, HPLC-grade solvents, were obtained from Merck (Darmstadt, Germany). Egg phosphatidylcholine (PC), cholesterol (Chol) and the fluorescent probes *N*-(7-nitro-benz-2-oxa-1,3-diazol-4-yl) phosphatidylethanolamine (NBD-PE), *N*-(Lissamine-rhodamine-B-sulfonyl)phosphatidylethanolamine (Rho-PE), 6,7 Br-PC, 9,10 Br-PC and 11,12 Br-PC were purchased from Avanti Polar Lipids (Birmingham, AL). Triton X-100 was obtained from Sigma (St. Louis, MO). All other reagents were of analytical grade. The spin-labelled phosphatidylcholine (1-acyl-2-[*n*-(4,4-dimethyloxazolidine-*N*-oxyl)] stearoyl-*sn*-glycero-3-phosphocholine, *n*-PCSL) with the nitroxide group at different positions, *n*, in the *sn*-2 acyl chain was also obtained from Avanti Polar Lipids. The spin-labels were stored at −20 °C in ethanol solutions at a concentration of 1 mg/ml.

2.2. Peptide synthesis

Peptides were synthesised by a solid-phase method using the Fmoc strategy and subsequently purified as previously reported [12]. The purified peptides were shown to be homogeneous (>98%) by analytical HPLC. The peptides were further subjected to electrospray mass spectroscopy to confirm their molecular weight. Peptide sequences are reported in Table 1.

2.3. Preparation of liposomes

Large unilamellar vesicles (LUVs) consisting of PC/Chol (55/45 w/w), and when necessary containing Rho-PE and NBD-PE, were prepared

Table 1
Peptide sequences.

Name	Sequence
HSV peptides	
gH626–644	GLASTLTRWAHYNALIRAF
gH776–802	STALLLFPNGTVIHLLAFDTQPVAAIA
gB168–186	VTVSQVWFGHRYSQFMGIF
gB632–650	PCTVGHRRYFTFGGGYVYF
Control peptides	
gp41-FP	AVGIGALFLGFLGAAGSTMGARS
Melittin	GIGAVLKVLTTGLPALISWIKRKRQQ

according to the extrusion method of Hope et al. [34] in 5 mM HEPES, 100 mM NaCl, pH 7.4. Lipids were dried from a chloroform solution with a nitrogen gas stream and lyophilized overnight. For fluorescence experiments, dry lipid films were suspended in buffer by vortexing; then the lipid suspension was freeze–thawed 6 times and then extruded 20 times through polycarbonate membranes with 0.1 μm diameter pores to produce large unilamellar vesicles.

Small unilamellar vesicles (SUVs) were prepared by sonication of PC/Chol (55/45 w/w) dispersions as previously described [35]. Briefly, dry lipid mixtures were dissolved in a $CHCl_3$/MeOH mixture (2/1 v/v). The solvents were then evaporated under a stream of nitrogen, and the lipids were subjected to a vacuum for at least 3 h and then resuspended in PBS buffer by vortexing. The resulting lipid dispersions were then sonicated for 10 min in a bath-type sonicator until clear.

Multilamellar vesicles (MLVs) of PC/Chol (55/45 w/w) to be used for ESR experiments were prepared by mixing appropriate amounts of solutions of PC in dichloromethane/methanol (2/1 v/v), Chol in chloroform, and spin-label solutions were mixed in small glass tubes. In all samples, the spin-label was 1% by weight of the total lipid mixture. A thin film of the lipid was produced by evaporating the solvent with a nitrogen gas stream. Final traces of solvent were removed by subjecting the sample to vacuum desiccation for at least 3 h. The samples were then hydrated with the appropriate buffer and vortexed.

2.4. Lipid mixing assays

Membrane lipid mixing was monitored using the resonance energy transfer assay (RET) reported by Struck et al. [36]. The assay is based on the dilution of the NBD-PE (donor) and Rho-PE (acceptor). Dilution due to membrane mixing results in an increase in NBD-PE fluorescence. Thus, we monitored the change in donor emission as aliquots of peptides were added to vesicles. Vesicles containing 0.6 mol% of each probe were mixed with unlabelled vesicles at a 1:4 ratio (final lipid concentration, 0.1 mM). Small volumes of peptides in dimethylsulfoxide (DMSO) were added; the final concentration of DMSO in the peptide solution was no higher than 2%. The NBD emission at 530 nm was followed with the excitation wavelength set at 465 nm. A cut off filter at 515 nm was used between the sample and the emission monochromator to avoid scattering interferences. The fluorescence scale was calibrated such that the zero level corresponded to the initial residual fluorescence of the labelled vesicles and the 100% value corresponding to complete mixing of all lipids in the system was set by the fluorescence intensity of vesicles upon the addition of Triton X-100 (0.05% v/v) at the same total lipid concentrations of the fusion assay. All fluorescence measurements were conducted in PC/Chol (55/45) LUVs. Lipid mixing experiments were repeated at least three times and results were averaged.

2.5. Binding analysis by surface plasmon resonance (SPR)

SPR experiments were carried out with a BIAcore 3000 analytical system (Biacore, Uppsala, Sweden) using HPA and L1 sensor chips. The HPA sensor chip contains hydrophobic alkanethiol chains, which are covalently bound to its gold surface, and a lipid heteromonolayer is created by introducing liposomes to the chip; the complete coverage of the surface with a polar lipid monolayer generates a membrane-like environment where analytes in aqueous buffer interact with a lipid monolayer [37]. The L1 sensor chip contains hydrophobic alkanethiol chains, with exposed polar headgroups, and a lipid bilayer is being created by introducing liposomes to the chip. The experimental protocol was previously described by Mozsolits et al. [25]. The running buffer used for all experiments was PBS (pH 7.4); the washing solution was 40 mM *N*-octyl β-D-glucopyranoside. All solutions were freshly prepared, degassed, and filtered through 0.22 μm pores. The operating temperature was 25 °C. After cleaning as indicated by the manufacturers, the BIAcore X instrument was left running overnight using Milli-Q water as eluent to thoroughly wash all liquid-handling parts of the instrument. The HPA (or L1) chip was then installed, and the alkanethiol surface was cleaned by an injection of the nonionic detergent *N*-octyl β-D-glucopyranoside (25 μl, 40 mM) at a flow rate of 5 μl/min. PC/Chol (55/45 w/w) SUVs (80 μl, 0.5 mM) were then applied to the chip surface at a flow rate of 2 μl/min. To remove any multilamellar structures from the lipid surface, we used NaOH 10 mM and increased the flow rate to 50 μl/min, which resulted in a stable baseline corresponding to the lipid monolayer (or bilayer in the case of L1) linked to the chip surface. The negative control BSA was injected (25 μl, 0.1 mg/μl in PBS) to confirm complete coverage of the nonspecific binding sites. Peptide solutions (30 μl at a flow rate of 5 μl/min) were injected onto the lipid surface. PBS alone then replaced the peptide solution for 15 min to allow peptide dissociation. SPR detects changes in the reflective index of the surface layer of peptides and lipids in contact with the sensor chip. A sensorgram is obtained by plotting the SPR angle against time. This change in the angle is then translated to response units. Analysis of the peptide–lipid binding event was performed from a series of sensorgrams collected at different peptide concentrations.

The sensorgrams for each peptide–lipid interaction were analysed by curve fitting using numerical integration analysis [38]. The BIA evaluation was used to perform complete kinetic analyses of the peptide sensorgrams. Several curve fitting algorithms were used but good fit was obtained only with the two-state reaction model, which was previously used for describing the possible binding mechanisms of antimicrobial peptides [19]. The data were fitted globally by simultaneously fitting the sensorgrams obtained at different peptide concentrations and the two-state reaction model was applied to each data set. This model describes two reaction steps [25] which, in terms of peptide–lipid interaction, may correspond to i) peptide (P) binds to lipids (L) to give PL and ii) the complex PL changes to PL*, which cannot dissociate directly to P + L and which may correspond to partial insertion of the peptide into the lipid bilayer.

$$P + L \underset{kd1}{\overset{Ka1}{\rightleftharpoons}} PL \underset{kd2}{\overset{ka2}{\rightleftharpoons}} PL^*.$$

The corresponding differential rate equations for this reaction model are represented where RU_1 and RU_2 are the response units for the first and second steps, respectively, C_A is the peptide concentration, RU_{max} is the maximum peptide binding capacity (or equilibrium binding response), and k_{a1}, k_{d1}, k_{a2}, and k_{d2} are the association and dissociation rate constants for the first and second steps, respectively.

$$dRU_1/dt = k_{a1} \times C_A \times (RU_{max} - RU_1 - RU_2) - k_{d1} \times RU_1 - k_{a2} \times RU_1 + k_{d2} \times RU_2 \quad (1)$$

$$dRU_2/dt = k_{a2} \times RU_1 - k_{d2} \times RU_2. \quad (2)$$

While k_{a1} has $M^{-1}\,s^{-1}$ units, k_{d1}, k_{a2}, and k_{d2} have s^{-1} units; thus the total affinity constant for the all process, K_A, has M^{-1} units. Kinetic

data were assessed by using χ^2 values, plots of the residuals from the model fitting and the significance of a parameter assessed by standard deviations. The quality of the fit to a specific parameter was deemed significant if the standard deviation was less than 10%. Except where specifically indicated, all parameter values were significant to the fit.

2.6. Tryptophan fluorescence experiments

Tryptophan is sensitive to its environment and has been previously utilised to evaluate peptide localization in the membrane. Emission spectra of the peptides containing at least one tryptophan residue (gH626–644, and gB168–186) in the absence or presence of target vesicles (PC/Chol = 55/45) were recorded between 300 and 400 nm with an excitation wavelength of 295 nm.

Br-PC employed as quencher of tryptophan fluorescence is suitable for probing membrane insertion of peptides, since it acts over a short distance and does not drastically perturb the membrane [39,40]. Peptides, containing the tryptophan residue, were added (final concentration of 0.5 μM) to 2 ml of buffer (5 mM HEPES, 100 mM NaCl pH 7.4) containing 20 μl (50 mM) of Br-PC/Chol SUV, thus establishing a lipid:peptide molar ratio of 100:1. After a 2 min incubation at room temperature, an emission spectrum of the tryptophan was recorded with excitation set at 295 nm. SUV composed of PC/Chol (55/45) and which contained 25% of either 6,7 Br-PC, or 9,10 Br-PC or 11,12 Br-PC were used. Three separate experiments were conducted for each peptide. In control experiments, peptides in PC/Chol (55/45) SUVs without Br-PC were used.

2.7. ESR spectroscopy

For ESR experiments, the suspension of PC/Chol (55/45) MLVs containing 1% by weight of a spin-labelled lipid, *n*-PCSL ($n = 5,7,10,14$), was transferred to a 100 μl glass capillary and pelleted in a tabletop centrifuge. Excess supernatant was removed and the capillary was flame sealed. Samples containing the peptides were prepared in a similar manner, except that the lipid film was hydrated directly with the peptide solution in buffer. The lipid:peptide mole ratio was set to 10:1. ESR spectra of lipid and lipid/peptide samples were recorded on a 9-GHz Bruker Elexys E-500 spectrometer, at 25 °C, using procedures and instrument setting reported in literature [41].

2.8. Circular dichroism measurements

CD spectra were recorded using a Jasco J-715 spectropolarimeter in a 1.0 or 0.1 cm quartz cell at room temperature. The spectra are an average of 3 consecutive scans from 260 to 195 nm, recorded with a band width of 3 nm, a time constant of 16 s and a scan rate of 10 nm/min. Spectra were recorded and corrected for the blank. Mean residues ellipticities (MRE) were calculated using the equation *Obsd*/*lcn*, where *Obsd* is the ellipticities measured in millidegrees, *l* is the length of the cell in centimetres, *c* is the peptide concentration in moles per litre, and *n* is the number of amino acid residues in the peptide. Solutions of peptides in SUVs (0.1 mM) were prepared as reported previously [11]. The peptide lipid ratios at which the experiments were performed is 0.1 and 0.5 (mole/mole).

3. Results

3.1. Selection of peptides

In order to investigate the mode of action of membranotropic peptides derived from the two HSV glycoproteins involved in the membrane fusion process (gB and gH), we have selected two peptides for each glycoprotein. For the glycoprotein H, the following peptides have been selected: gH626–644, the putative internal fusion peptide of gH [11]; and gH776–802, corresponding to the pre-transmembrane domain [12]. The two peptides that have been selected for the glycoprotein B were shown in a previous work [15] to have the highest fusion activity as well as inhibitory activity; in particular, gB168–186 corresponds to one of the two fusion loops predicted from the analysis of the crystallographic structure [9] while the other peptide gB632–650 is located in the most hydrophobic C-terminal domain of gB. A shorter version of this latter peptide, namely gB636–650, has been recently confirmed to have antiviral activity [42].

In our experiments we also used two control peptides: melittin and HIV fusion peptide (gp41-FP). In particular, melittin is the major component of the venom of the honey bee *Apis mellifera* and has been extensively characterised by other groups [43]. On the other hand, the fusion peptide of HIV [44], which has never been analysed by SPR, has been chosen in order to compare our data with those obtained for a well-known viral fusion peptide.

3.2. Fusogenic ability of peptides

The fusogenic activity of the HSV peptides has been reported previously [11,12,15]. Here, we compare the fusion activity obtained for the HSV peptides in PC/Chol 55/45 with that obtained for the control peptides melittin and gp41-FP; this comparison is necessary since the fusion activity of melittin and gp41-FP has never been reported in the experimental condition used for HSV peptides. The fusion activity has been determined by their ability to cause lipid mixing of large unilamellar vesicles (LUVs). A population of LUVs labelled with both NBD-PE and Rho-PE was mixed with a population of unlabelled LUVs in the presence of increasing concentrations of peptides. Fusion between the labelled and unlabelled vesicles caused by the peptides results in dilution of the labelled lipids and therefore reduced energy transfer between NBD-PE and Rho-PE. This change can be visualised as an increase of NBD fluorescence.

We already discussed in a previous paper [15] that although the use of peptide fragments might not mimic the properties of the intact protein, peptide studies give an indication of the relative propensities of the different domains implicated in the fusion process. Fig. 1 shows the results obtained for all the peptides used in this paper. In particular, gB632–650 and melittin already show a high fusion activity at the lowest peptide to lipid ratio tested ([Peptide]/[Lipid] = 0.05, fusion of 20–25%) (mole/mole), while the other four peptides all show a lower activity at the same ratio. Among the other four peptides, gH626–644 and gp41-FP considerably increase their fusogenic activity at higher peptide concentrations and reach high fusion levels at a peptide/lipid ratio of 0.5. It is noteworthy that gB168–186, one of the two N-terminal fusion loops of the

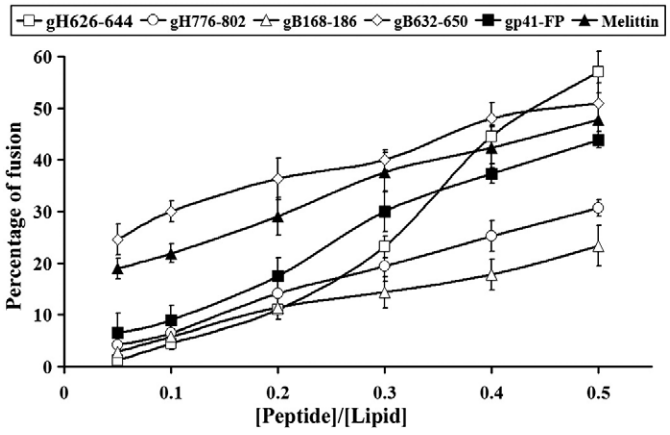

Fig. 1. Peptide-promoted membrane fusion of PC/Chol (1:1) LUVs as determined by lipid mixing; peptide aliquots were added to 0.1 mM LUVs, containing 0.6% NBD and 0.6% Rho. The increase in fluorescence was measured after the addition of peptide aliquots; reduced Triton X-100 (0.05% v/v) was referred to as 100% of fusion.

glycoprotein gB, has an apparently lower fusion activity than the other peptides. This result might be due to the fact that this loop acts as a part of a bipartite fusion domain to induce fusion.

3.3. Binding affinity of the peptides to lipid monolayers and bilayers measured by SPR

We utilised a BIAcore biosensor method to investigate the mode of action of membranotropic peptides.

PC/Chol monolayers and bilayers were absorbed onto the HPA and L1 chips, respectively. Sensorgrams of the binding of all the peptides are shown in Figs. 2 and 3. The sensorgrams revealed that the RU signal intensity increased as a function of the peptide's concentration. This indicates that the amount of peptide bound to the lipids is proportional to the peptide concentration. The sensorgrams of the binding of melittin with lipid monolayers showed markedly lower response levels as compared with its binding to bilayers. In contrast, all the other peptides showed a similar response to monolayers as compared to bilayers. The inspection of the shape of each sensorgram reveals different binding kinetics with significant differences both among the peptides and between the two different lipid surfaces. In particular, the sensorgrams obtained for the L1 chip indicate that most of the peptides bind to the lipid surfaces in a biphasic manner. The initial association starts as a fast process and then slows down considerably towards the end of the peptide injection. The dissociation follows a similar pattern, with the signal falling rapidly at the end of injection since the peptide is no longer present and the buffer flow removes a large amount of free or weekly bound peptide,

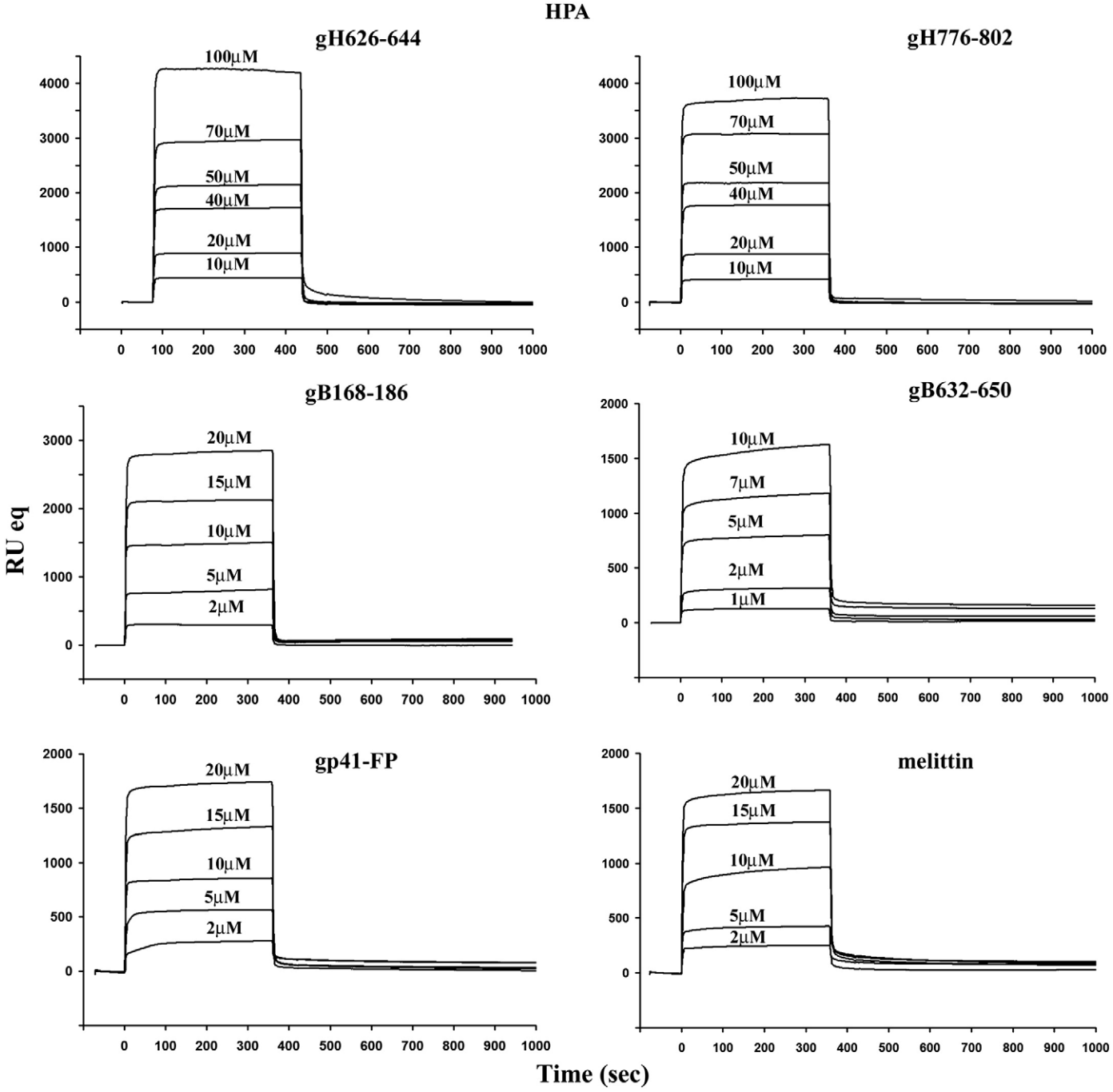

Fig. 2. Sensorgrams of the binding of gH626–644 (A), gH776–802 (B), gB168–186 (C), gB632–650 (D), gp41-FP (E) and melittin (F) with the monolayers PC/Chol (HPA chip).

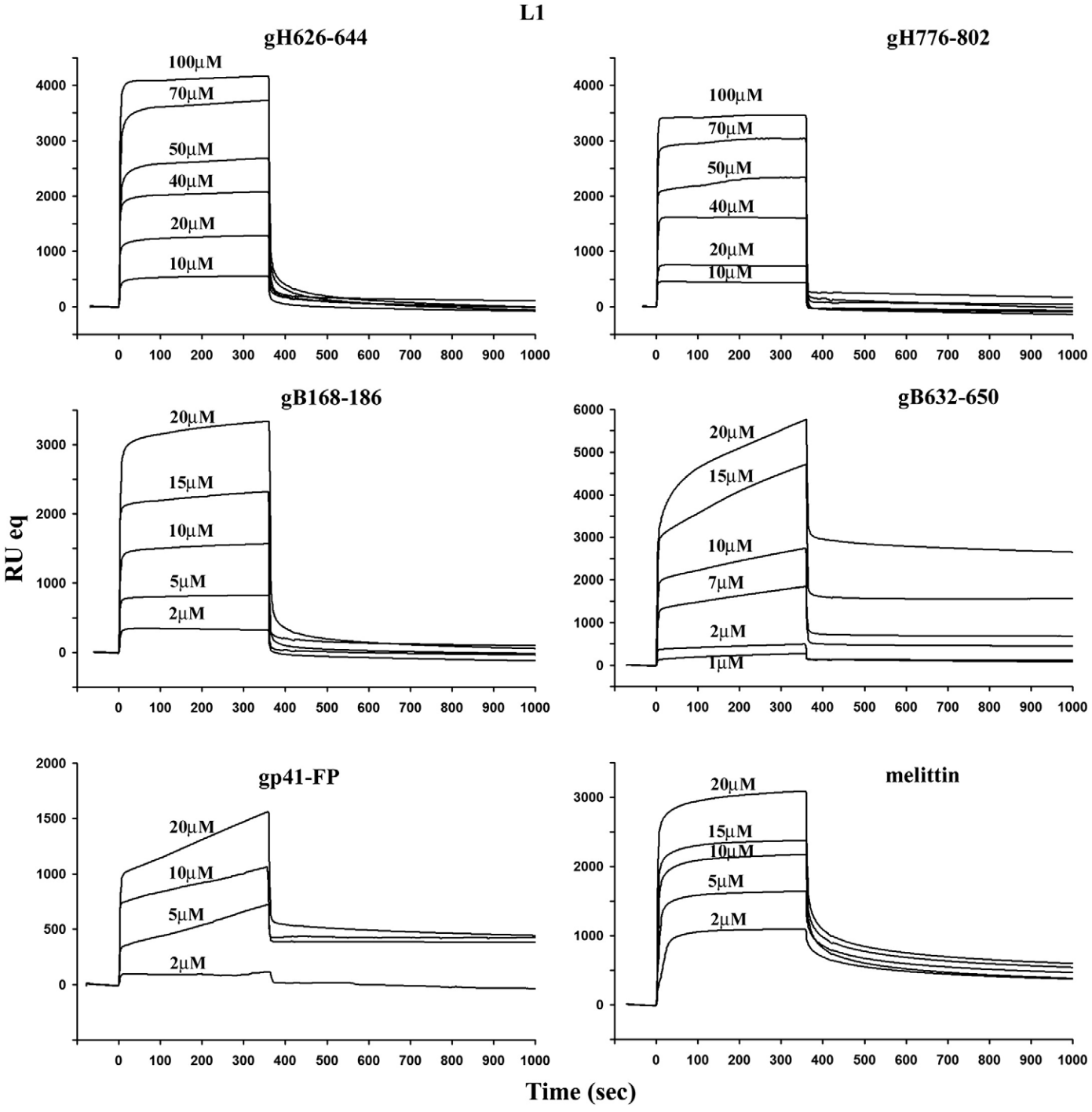

Fig. 3. Sensorgrams of the binding of gH626–644 (A), gH776–802 (B), gB168–186 (C), gB632–650 (D), gp41-FP (E) and melittin (F) with the bilayers PC/Chol (L1 chip).

followed by a much slower step. In particular, the sensorgrams for gB632–650, gp41-FP and melittin clearly indicate a change in the association with a second much slower association step evident in the L1 chip compared to the HPA chip. Moreover, their sensorgrams did not return to zero on the L1 chip, indicating that the peptides remained significantly bound to the surface or inserted into the hybrid bilayer membrane.

We employed numerical integration analysis that uses nonlinear analysis to fit an integrated rate equation directly to the sensorgrams [28]. When fitting the peptide's sensorgrams globally (using different concentrations of the peptides) with the simplest 1:1 Langmuir binding model, a poor fit was obtained ($\chi^2 > 100$), confirming that this model does not represent the lipid binding mechanism of all the peptides investigated. However, a significantly improved fit was obtained using numerical integration of the two-state reaction model of the binding sensorgrams, suggesting that there is likely to be at least two steps involved in the interaction between the peptide and hybrid bilayer membrane surface. In analogy with previous studies of peptide–membrane interactions using SPR [19], the first step may correspond to the actual binding of the peptide to the surface, and the second step to the insertion of the peptide into the hydrophobic core of the membrane. A set of peptide sensorgrams with different peptide concentrations was used to estimate the kinetic parameters. The average values for the rate constants obtained from the two-state model analysis are listed in Tables 2 and 3 along with the affinity constant values (K_A). The data in Tables 2 and 3, clearly indicate the

Table 2
Association (k_{a1}, k_{a2}) and dissociation (k_{d1}, k_{d2}) rate constants obtained for the HPA chip using the two-state model.

	k_{a1}	k_{d1}	K_1	k_{a2}	k_{d2}	K_2	K_A
gH626–644	$(8.14\pm0.02)10^2$	$(4.39\pm0.05)10^{-2}$	$1.8\ 10^4$	$(6.40\pm0.07)10^{-4}$	$(2.13\pm0.04)10^{-4}$	3.0	$7.42\ 10^4$
gH776–802	$(9.80\pm0.05)10^1$	$(6.77\pm0.02)10^{-2}$	$1.4\ 10^3$	$(4.37\pm0.03)10^{-2}$	$(5.83\pm0.08)10^{-3}$	7.5	$2.42\ 10^4$
gB168–186	$(7.40\pm0.03)10^1$	$(3.81\pm0.03)10^{-3}$	$1.9\ 10^4$	$(2.05\pm0.02)10^{-2}$	$(1.65\pm0.01)10^{-2}$	1.2	$4.35\ 10^4$
gB632–650	$(3.16\pm0.06)10^2$	$(5.73\pm0.03)10^{-3}$	$5.5\ 10^4$	$(5.28\pm0.02)10^{-3}$	$(1.71\pm0.01)10^{-3}$	3.1	$2.25\ 10^5$
Melittin	$(8.60\pm0.03)10^1$	$(7.93\pm0.01)10^{-3}$	$1.1\ 10^4$	$(1.41\pm0.05)10^{-3}$	$(1.83\pm0.09)10^{-3}$	0.8	$1.92\ 10^4$
gp41-FP	$(1.03\pm0.02)10^2$	$(5.69\pm0.01)10^{-3}$	$1.8\ 10^4$	$(2.88\pm0.04)10^{-3}$	$(1.18\pm0.05)10^{-4}$	24.4	$4.62\ 10^5$

The affinity constants K_1 and K_2 are for the first ($K_1 = k_{a1}/k_{d1}$) and for the second ($K_2 = k_{a2}/k_{d2}$) steps respectively, and the affinity constant (K_A) determined as $(k_{a1}/k_{d1})\times(k_{a2}/k_{d2})$ is for the complete binding process. Standard deviations are reported in brackets.

main influence on the overall binding constant of the fast association rate and slow dissociation rate of the first step. If this step corresponds to the electrostatic interaction, these results clearly indicate that electrostatic forces play an important role in the binding of membrane-active peptides.

Analysis of data reported in Tables 2 and 3 allowed several important observations. The difference between the affinity of the peptides to HPA chips as compared to L1 chips should indicate the contribution of the inner leaflet to the binding process [28,45–47]. In fact, due to structural differences between supported monolayers (HPA chip) and immobilised liposomes (L1 chip), it is possible to differentiate between the surface adsorption and/or partial insertion in the HPA chip and complete insertion into the hydrophobic core of the membrane in the liposomes of the L1 chip. The values of the ratio $K_{A\ bilayer}/K_{A\ monolayer}$, listed in Table 4, demonstrates that the binding of melittin to bilayers is approximately 36-fold higher than to monolayers, indicating that it is inserted deeply into the inner membrane and thus supporting the pore-forming property of melittin. Data obtained using the peptide melittin are in good correlation with those reported by others [48,49]. In particular we obtained a binding affinity of approximately 10^4 with a higher affinity for the bilayer than the monolayer; our binding affinities are slightly lower than those previously reported [48,49] probably due to the different lipid composition used in our study, which was selected according to previous data collected by our group on HSV-1 peptides induced fusion of liposomes [11].

The first interesting observation is the different behaviour of HSV peptides and of the HIV fusion peptide from the melittin, indicating a different mechanism of action. The values of the ratio $K_{A\ bilayer}/K_{A\ monolayer}$ (Table 4) demonstrate that the binding of the HSV peptides as well as the HIV fusion peptide to monolayers, is similar to their binding to bilayers, indicating that the peptides are not influenced by the membrane's inner leaflet. Thus, our result supports the hypothesis that viral peptides equally interact with the inner and outer leaflet stably inserting into the PC/Chol membrane.

The analysis of binding constants reveals that the peptides gH776–802 and gB168–186 are the ones with the lowest affinity for both bilayers and monolayers. gH776–802 represents a hydrophobic peptide with membranotropic characteristics that has been derived from the pre-transmembrane domain of gH, therefore, it is not supposed to behave like canonical fusion peptides, instead it is conceivable its putative activity in strengthening the interaction between opposing membranes during fusion. In this respect, the SPR results demonstrate an involvement of this peptide in a superficial interaction with lipids, and this is further supported by the fact that gH776–802 shows a comparable affinity constant for the monolayer and for the bilayer. gB168–186 is only a part of the bipartite fusion peptide of gB, that is composed of two loops [9], and although showing a significant fusion activity and interaction with the bilayer it's activity is lower than that of the other membrane interacting peptides.

gp41-FP, gB632–650 and gH626–644 can be grouped as the peptides with a higher binding constant for both monolayers and bilayers. This result is of great importance because gp41-FP is the well-known HIV-1 fusion peptide, gB632–650 is located in an outer β-strand of domain IV of the glycoprotein gB, which contributes many of the essential trimer contacts; and we previously reported [15] that it has the features of a membranotropic peptide, while gH626–644 is a putative internal fusion peptide of gH. The role of gH in fusion is still debated and since a crystallographic structure is missing, the recognition of further characteristics of gH626–644 could be valuable. These findings, demonstrating a stable insertion of the gH peptide into the membrane and complemented by previous data such as gH626–644 ability to fuse liposomes with high efficiency, its plasticity, the non accessibility to proteolitic cleavage once bound to membranes, the amphipathic character, the high hydrophobicity and high α-helical content determined by CD and NMR, makes of gH626–644 a likely candidate as the most fusogenic region of gH [11,13,14].

The analysis of the results obtained for the peptide gB632–650, the host hydrophobic C-terminal region of gB, demonstrates that also this peptide behaves similarly to the HIV fusion peptide. In particular, gB632–650 strongly binds to the vesicles and at the highest concentration used it irreversibly binds to both the monolayer and the bilayer. In the sensorgrams obtained with the L1 chip we detect a strong effect also at low concentrations, indicating a deep insertion of the peptide inside the bilayer.

3.4. Tryptophan fluorescence experiments

A tryptophan residue naturally present in the sequence of a protein or a peptide can serve as an intrinsic probe for the localization of the peptide within a membrane. Peptides gH626–644 and gB168–186 contain a tryptophan residue in the middle of the sequence; in particular it is the 9th residue in gH626–644 and the 7th residue in

Table 3
Association (k_{a1}, k_{a2}) and dissociation (k_{d1}, k_{d2}) rate constants obtained for the L1 chip using the two-state model.

	k_{a1}	k_{d1}	K_1	k_{a2}	k_{d2}	K_2	K_A
gH626–644	$(5.23\pm0.09)10^2$	$(4.38\pm0.08)10^{-2}$	$1.2\ 10^4$	$(2.41\pm0.02)10^{-3}$	$(3.98\pm0.07)10^{-3}$	0.6	$6.92\ 10^4$
gH776–802	$(4.2\pm0.01)10^1$	$(1.09\pm0.03)10^{-3}$	$4.2\ 10^4$	$(2.73\pm0.02)10^{-4}$	$(1.96\pm0.03)10^{-3}$	0.1	$2.30\ 10^4$
gB168–186	$(4.83\pm0.09)10^2$	$(6.28\pm0.03)10^{-2}$	$7.7\ 10^3$	$(3.77\pm0.04)10^{-3}$	$(4.21\pm0.02)10^{-3}$	0.9	$1.46\ 10^4$
gB632–650	$(9.9\pm0.02)10^1$	$(3.17\pm0.01)10^{-3}$	$3.1\ 10^4$	$(4.85\pm0.01)10^{-3}$	$(5.00\pm0.03)10^{-4}$	9.7	$3.94\ 10^5$
Melittin	$(4.85\pm0.02)10^3$	$(1.75\pm0.02)10^{-2}$	$2.8\ 10^5$	$(3.55\pm0.04)10^{-3}$	$(2.33\pm0.02)10^{-3}$	1.5	$7.01\ 10^5$
gp41-FP	$(3.2\pm0.07)10^1$	$(1.92\pm0.09)10^{-4}$	$1.6\ 10^5$	$(1.11\pm0.02)10^{-5}$	$(1.30\pm0.09)10^{-5}$	0.8	$3.53\ 10^5$

The affinity constants K_1 and K_2 are for the first ($K_1 = k_{a1}/k_{d1}$) and for the second ($K_2 = k_{a2}/k_{d2}$) steps respectively, and the affinity constant (K_A) determined as $(k_{a1}/k_{d1})\times(k_{a2}/k_{d2})$ is for the complete binding process. Standard deviations are reported in brackets.

Table 4
Binding to bilayers versus monolayers.

Peptides	$K_{bilayer}/K_{monolayer}$
gH626–644	0.9
gH776–802	1.0
gB168–186	0.3
gB632–650	0.9
Melittin	36
gp41-FP	0.8

gB168–186. The fluorescence emission of a tryptophan residue increases when the amino acid enters a more hydrophobic environment, and together with an increase in quantum yield, the maximal spectral position is expected to be shifted toward shorter wavelengths (blue shift). Fig. 4 shows the fluorescence emission spectra of the peptides gH626–644 and gB168–186 upon interaction with PC/Chol vesicles. In both cases changes in the spectral properties of the peptides were observed, suggesting that the tryptophan residue of the two peptides is located in a less polar environment upon interaction with lipids.

Furthermore, the position of the peptides inside the bilayer can be investigated by measuring the relative quenching of the fluorescence of the trp residue by the probes 11,12-Br-PC, 9,10-Br-PC and 6,7-Br-PC, which differ in the position of the quencher moiety along the hydrocarbon chain and permit to establish the depth of the peptide in the membrane by comparing the quenching results obtained with each of them. 6,7-Br-PC is a better quencher for molecules near or at the interface, while the other two are better probes for molecules buried deeply in the membrane. With both peptides the largest quenching of tryptophan fluorescence was observed with 11,12-Br-PC vesicles (Table 5). Slightly less quenching was observed with 9,10-Br-PC, and 6,7-Br-PC. These results indicate that, upon binding to vesicles, the peptides were inserted into the membrane bilayer.

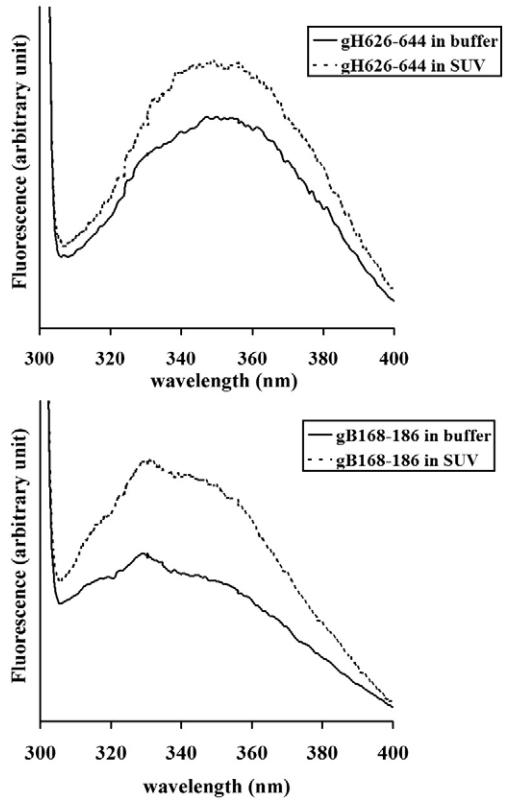

Fig. 4. Tryptophan fluorescence spectra in buffer and in liposomes for gH626–644 (panel A) and gB168–186 (panel B).

Table 5
Fluorescence intensity of peptides in bromolipid vesicles.

	Peptides	
Lipid	**gH626–644**	**gB168–186**
PC/Chol	100	100
6,7-Br-PC/Chol	84 ± 5	66 ± 7
9,10-Br-PC/Chol	68 ± 3	76 ± 8
11,12-Br-PC/Chol	64 ± 4	51 ± 6

The fluorescence is reported as a percentage of the fluorescence in PC/Chol. Standard deviations calculated on three independent measurements are reported.

3.5. ESR investigation on the interactions between fusion peptides and PC/Chol membranes

The ESR spectroscopy, by using spin-labelled substances (peptides and/or lipids) has been proved to give substantial information on the interaction between viral fusion peptides and lipid membranes [32,33]. In the present work, the association of the four peptides under investigation with lipid bilayers was investigated by analysing changes in ESR spectra of spin-labelled lipids, as reported in the literature for other peptides derived from viral fusion proteins [41,50,51] as well as for classical water-soluble peripheral membrane proteins [30,52–55]. The samples investigated were phosphatidylcholine spin-labelled at different positions, *n*, in the *sn*-2 chain (*n*-PCSL, $n = 5, 7, 10, 14$) incorporated in PC/Chol membranes (55/45 w/w), in the presence of the peptides. Preliminarily, the spectra in the absence of the peptides were also registered. Inspection of Fig. 5 shows that all the spectra present a clearly defined axially anisotropic lineshape, an evidence that, due to the high cholesterol content, the PC/Chol bilayer is in the liquid-ordered state [56]. In an attempt to quantitatively analyse the spectra, the order parameter, *S*, was calculated according to the relation [57]:

$$S = \frac{(T_{\parallel} - T_{\perp})}{(T_{zz} - T_{xx})} \frac{a_N}{a'_N} \tag{3}$$

where $T_{\parallel}$ and $T_{\perp}$ are two phenomenological hyperfine splitting parameters which can be determined experimentally for each spin-labelled phospholipid as shown in Fig. 5 (note that $2T'_{\perp} = 2T_{\perp} - 1.6$) [58]. T_{xx} and T_{zz} are the principal elements of the real hyperfine splitting tensor in the spin Hamiltonian of the spin-label, which can be measured from the corresponding single-crystal ESR spectrum and are reported in the literature ($T_{xx} = 6.1$ G and $T_{zz} = 32.4$ G) [59]. a_N and a'_N are the isotropic hyperfine coupling constants for the spin-label in crystal state and in the membrane, respectively, given by:

$$a_N = \frac{1}{3}(T_{zz} + 2T_{xx})$$

$$a'_N = \frac{1}{3}(T_{\parallel} + 2T_{\perp})$$

The isotropic hyperfine coupling constant is an index of the micropolarity experienced by the nitroxide, and the a_N/a'_N ratio in Eq. (3) corrects the order parameter for polarity differences between the crystal state and the membrane. Both *S* and a'_N decrease progressively with increasing *n*, as the spin-label position is stepped down the chain toward the center of the membrane, see Fig. 6. The *S* variation is an evidence of the flexibility gradient in segmental chain mobility [32,60], indicating that the lipid bilayer presents a relatively rigid surface and rigid interior [61–63]. The a'_N decrease is related to the polarity gradient [33], indicating that the hydrophobicity increases as the nitroxide group moves to the center of the bilayer. Association of peptides to the lipid bilayer causes a significant variation in the ESR spectra of spin-labelled phospholipids. As an example, Fig. 5 gives the ESR spectra of *n*-PCSL in PC/Chol bilayer

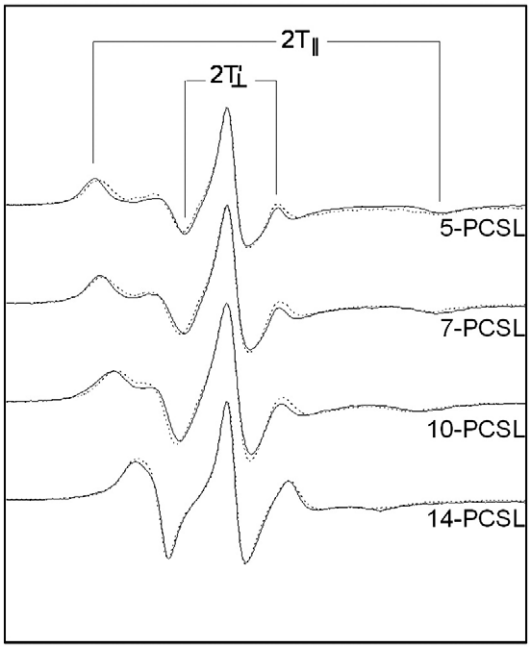

Fig. 5. ESR spectra of *n*-PCSL positional isomers in PC/Chol membranes in presence (solid line) and absence (dashed line) of gH626–644.

membranes, in the presence and absence of gH626–644 at a lipid: peptide molar ratio of 10/1. The presence of the gH626–644 induces slight but significant changes in the spin-label ESR spectra, which are mainly detectable from the low- and high-field component position and lineshape.

In an attempt to quantify these evidence, the S and a'_N values were determined. Fig. 6 shows the dependence of these parameters on chain position, n, for the *n*-PCSL spin-labels in PC/Chol membranes, in the absence and in the presence of the peptides. In all cases, the flexibility and polarity gradients with the chain position of the lipid bilayer membranes are preserved. Concerning a'_N, it appears that its value is only marginally affected by the peptides, i.e., no evident variation in the local polarity is detectable. In contrast, inspection of panel A of the figure reveals significantly different behaviour of the lipid chain mobility in the presence of the various peptides. In the same figure the S variation with respect to the value determined in the absence of any peptide, ΔS, is also reported. In the case of gH776–802, addition of a peptide does not significantly affect the S value at any chain position. In the case of gB168–186, ΔS decreases – almost tending to zero – with increasing n. gH626–644 causes an increase in S to a comparable extent at all chain positions. The perturbations due to gB632–650 increase with n. This indicates that the increase in lipid packing density, which is induced by insertion of gH626–644, and even more by that of gB632–650, propagates down the chain more effectively than for the other peptides.

It is interesting to compare these results with those obtained for the two reference peptides, namely gp41-FP and melittin. In the case of gp41-FP, the spin-labels presenting the nitroxide group in position $n = 5, 7, 10$ present a clearly detectable S increase, as shown in Fig. 6. Strikingly, for what concerns the spin-label presenting the nitroxide in a deeper position, 14-PCSL, the presence of gp41-FP causes the appearance of a second component in the ESR spectrum, see Fig. 7. The second component is resolved in the outer wings of the spectrum and corresponds to spin-labelled lipid chains whose motion is restricted. This is a feature already encountered for all the peptides and proteins which stably inserts in the lipid bilayer, such as integral membrane proteins [30]. The slow motional component is due to spin-labelled lipids participating to the "annular" structure surrounding the guest molecule, while the fluid component is due to relatively unperturbed spin-labels in bulk lipid. Thus, we can conclude that gp41-FP deeply inserts into the lipid bilayer. A similar experimental evidence has been found by Curtain et al. for the same peptide in egg yolk phosphatidylcholine [33]. In this context, it is relevant to note that the same authors, by analysing ESR spectra of spin-labelled gp41-FP in lipid bilayers, concluded that the membrane-bound peptide could self-aggregate [32].

In the presence of melittin, the S increases to a comparable extent at all chain positions, similarly to that already reported in the literature by using different lipid bilayers [64]. However, no second component in the ESR spectra can be observed, at any n position of the spin-label acyl chain. This evidence has been found in all cases where peptides or proteins interact with the more external part of the bilayer, inducing a lipid chain perturbation that propagates to the inner part of the membrane [54]. Interestingly, similar results have also been recently obtained for a peptide derived from the pre-transmembrane region of the FIV gp36 glycoprotein, which induces a destabilisation of lipid bilayers [41], thus supporting the view that ESR alone is unable to discriminate between lytic and membranotropic domains.

Concerning the peptides analysed in the present work, analysis of Fig. 7 shows that, while gH626–644 only causes an enlargement of the spacing between the two more external signals, i.e. an S increase, in the case of gB632–650 the appearance of a shoulder at low field and of a broad minimum at high field suggest a behaviour more similar to that of gp41-FP. Thus, these experimental evidence indicate that gH626–644 interacts with the lipid bilayer being located in the more external part of it. In contrast, gB632–650 deeply penetrates in the bilayer, stably inserting into its inner region.

3.6. Secondary structure of synthetic peptides

Since the structural conformation of peptides has been shown in many cases to correlate with fusogenic activity, and to understand whether secondary structure induction contributes to the initial stages of peptide binding, the secondary structure of the four HSV peptides and of the two control peptides in buffer and in PC/Chol 55/45 SUVs was determined by CD spectroscopy (Fig. 8). As reported in literature [44], fusion peptides may change their secondary structure at different peptide/lipid ratios, in particular, they may show a beta and/or oligomeric structure at high peptide/lipid ratios, while they may assume an α-helical structure at low peptide/lipid ratios.

The secondary structure measurements for each peptide were thus performed at two different peptide/lipid ratios; in particular, we used a molar ratio of 0.1 (low peptide/lipid ratio) and a ratio of 0.5 (high peptide/lipid ratio). The ratio of 0.5 was tested because in this condition we could clearly evidence a high fusion activity for all the peptides. All the spectra shown in Fig. 8 for the 6 peptides are indicative of the formation of substantial secondary structure in PC/Chol. The melittin shows an helical spectrum in buffer and at both ratios with minima at 222 nm and 208 nm. The spectra for the peptide gp41-FP is consistent with the formation of a predominantly β-sheet conformation at high peptide/lipid ratios and an helical structure at low peptide/lipid ratios, as already reported for this peptide at the same ratios [44]. The spectra for the peptide gH626–644 is consistent with a predominantly α-helical conformation. All the other peptides show spectra consistent with a predominantly β-sheet conformation in the condition tested.

4. Discussion

Peptide–membrane interactions play a central role in numerous biological processes and are characterised by several complex and still unknown steps. In fact, it is likely that membranotropic peptides initially bind to the bilayer surface through mainly electrostatic

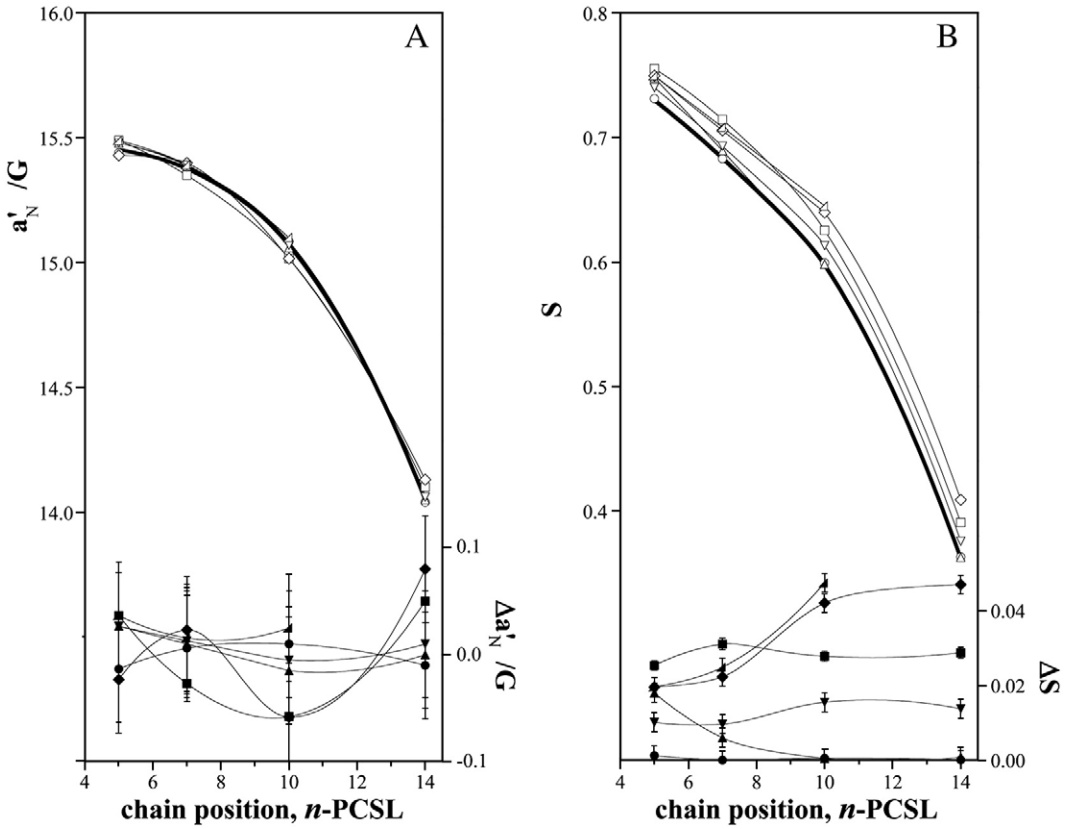

Fig. 6. Dependence on spin-label position, *n*, of the isotropic hyperfine coupling constant, a'_N (panel A, left-hand ordinate), and of the order parameter, *S* (panel B, left-hand ordinate), of the *n*-PCSL in PC/Chol in the absence (bold line) and in the presence of gH626–644 (□), gH776–802 (○), gB168–186 (△), gB632–650 (◊), melittin (▽) or gp41-FP(◿). T = 25 °C. Variation of a'_N (panel A, right-hand ordinate), and *S* (panel B, right-hand ordinate) with respect to the unperturbed bilayer, on adding gH626–644 (■), gH776–802 (●), gB168–186 (▲), gB632-650 (♦), melittin (▼) or gp41-FP (◢) to the membrane.

interactions, then assume a particular secondary structure and eventually insert into the lipid membrane. The exact mechanism of interaction is supposed to play a fundamental role in the activity of the peptide. Conformational and binding properties represent key aspects of the interaction that may help in understanding the factors that contribute to the binding of membrane-active peptides to biomembranes. The present study demonstrates that SPR is a powerful tool for investigating real-time interactions between membranotropic peptides and lipid monolayers and bilayers, and as a result, allows distinguishing between different modes of action. This is because it allows continuous monitoring of two major steps: the initial association to the membrane and the slower insertion into the hydrophobic core.

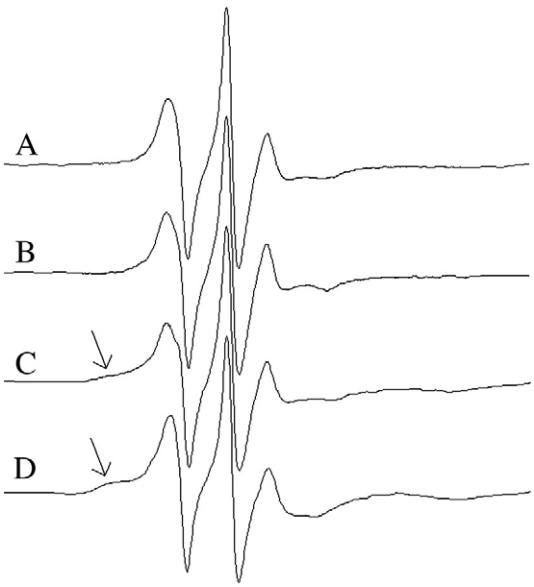

Fig. 7. ESR spectra of 14-PCSL positional isomers in PC/Chol membranes in the absence (A) and presence of gH626–644 (B), gB632–650 (C) and gp41-FP (D). Arrows indicate the position of the second, more immobilised, spectral component.

We used four synthetic peptides corresponding to the known membrane interacting regions of HSV fusion glycoproteins gH and gB, namely gH626–644, gH776–802, gB168–186 and gB632–650. In particular, gH626–644 has been previously identified as the putative fusion peptide of gH [11,65,66], while gH776–802 corresponds to the pre-transmembrane domain of gH and has been shown to interact significantly with liposomes and thus to be involved in the fusion process [12]. gB168–186 of HSV gB has been identified by other methodologies as a fusion peptide [9,15], while gB632–650 has also been previously shown to interact with membranes and to have a significant inhibitory activity [15,42]. As control peptides we used the fusion peptide of HIV and melittin, a cationic antimicrobial peptide; the HIV fusion peptide was selected to determine the behaviour of a peptide able to stably interact with membranes at a certain depth, while melittin was selected as being responsible for the formation of pores through the bacterial membrane. We followed the binding of the peptides to both the monolayer and the bilayer membranes and this allowed us to examine the contribution of the inner leaflet of the membrane with regard to the binding properties of viral membranotropic peptides. This approach was recently reported for discriminating between transmembrane pore formation versus membrane perturbation.

The SPR data show a marked difference between the mode of action of the HSV peptides and the HIV fusion peptide compared to

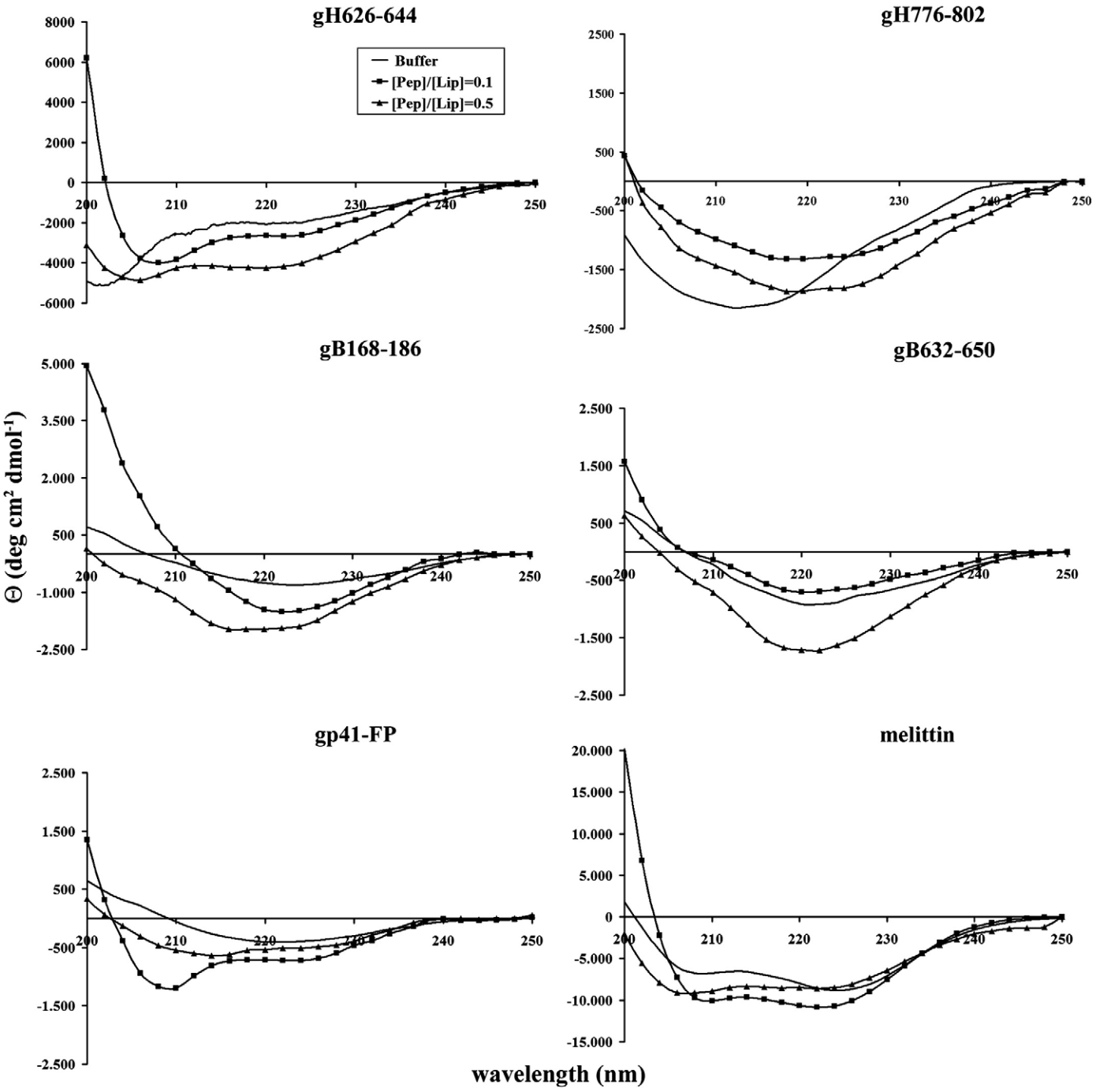

Fig. 8. Circular dichroism spectra of peptides in buffer and in PC/Chol at different peptide/lipid (mole/mole) ratios.

melittin, suggesting that viral-derived membrane interacting peptides all act via a similar mechanism, which is substantially different from that of the non-cell selective lytic peptide melittin. Tables 2 and 3 show that for all the gH and gB peptides as well as the HIV fusion peptide, there is almost no difference between the affinity to monolayers as compared to bilayers. This indicates that the outer and inner leaflets equally participate in the binding, or in other words, the peptides stably insert into the PC/Chol membrane but they are unable to form pores. Thus, our results strongly suggest that all the analysed peptides penetrate into the hydrophobic core of the membrane at variable depths without forming pores and therefore their fusion activity may be due to their insertion inside the bilayer which causes the perturbation of the packing of the lipids and a differential surface area increase of the outer and inner membrane leaflets which are responsible of starting the fusion process.

From the analysis of the data obtained for the various peptides, we were able to better understand the different behaviour of membranotropic sequences. The peptide gH776–802 shows only a superficial interaction with the membranes, thus suggesting that it probably is only marginally involved in the fusion process. This is consistent with its putative support action in the overall fusion mechanism. The peptide gB168–186 penetrates slightly into the membrane bilayer; its fusion activity and the binding constants are lower than that of other fusion peptides, the fluorescence experiments show that the

tryptophan (that is in the middle of the sequence) is located inside the membrane bilayer, but ESR studies show a superficial interaction of the peptide with the membrane; its behaviour may be due to the intrinsic properties of a bipartite fusion peptide, where only the contemporary presence of both peptides is able to perturb the lipid bilayers.

Nevertheless, the other two HSV peptides, namely gH626–644, and gB632–650 strongly interact with both membrane models with an affinity constant similar to the one obtained for HIV gp41 fusion peptide (gp41-FP). This novel result point to a clear distinction between the behaviour of viral fusion peptides and other membranotropic peptides. By ESR experiments, we were able to differentiate between the three most active peptides: gH fusion peptide gH626–644 and the gB peptides gB168–186 and gB632–650. In fact, gH626–644 and even more evidently gB632–650 are able to deeply enter the lipid bilayers similarly to gp41-FP.

There have been numerous structure studies on fusion peptides but there is not yet a clear correlation between structure and fusogenic activity; in particular, fusion peptide can adopt either helical or β-strand conformation. An α-helix conformation has been proposed to be associated with pore formation by peptides in vesicle membranes [67,68], while the extended antiparallel β-structure of the peptides was believed to be involved in the initial steps of the fusion process, being likely to reside primarily at the lipid–water interface; in most studies on viral fusion peptides an α-helical arrangement of the lipid-bound peptide has also been suggested to represent the fusion-active conformation [44,69]. CD data reveal that melittin can adopt an α-helical conformation in all the experimental conditions that we tested here and that the monomer/oligomer equilibrium is shifted toward the oligomeric state; the peptide gH626–644 shows a high α-helical content although it does not show oligomerization phenomena in the condition tested here, while all the other peptides show a β-structure. Our results favour the involvement of peptides in a β-conformation in the actual fusion event, although we cannot eliminate the possibility that fusion peptides may adopt an α-helix conformation when more deeply inserted inside the bilayer. A dynamic equilibrium between helix and non-helix forms of the fusion peptide in the membrane environment appears thus to be essential for the fusion process. The secondary structure of fusion peptides may be of importance in the interaction with the membrane and involves both electrostatic and hydrophobic effects; in fact, fusion peptides could be adsorbed at the membrane interface and change their conformation adopting a beta and/or aggregate structure as a consequence of the different lipid headgroups present in the bilayer. Moreover when in an helical conformation they could be inserted more deeply than the membrane interface.

We have also shown that the combination of SPR and ESR is a powerful tool to obtain real-time monitoring of the steps governing the mode of action of membrane-active peptides, some of which could not be detected directly by other means. The SPR studies clearly differentiate between the two steps involved in membrane binding and permeation via the two general mechanisms, namely, pore formation by melittin and membrane insertion for all the other peptides. In this respect, it is outstanding that the $K_{bilayer}/K_{monolayer}$ for melittin is very high compared to the others, clearly discriminating the pore formation from other membrane insertion mechanisms that may either involve an α-helix or a β-sheet conformation. Thus, membrane location rather than conformation may discriminate between fusion peptides and other membranotropic sequences. Partial peptide insertion into the outer leaflet of the target cell membrane would likely perturb the leaflet and lead to fusion.

To the best of our knowledge, this is the first report that, using in combination ESR and SPR, has been applied to study viral fusion peptide interactions with membranes. Although affinity constants and lipid insertion capabilities are not the sole properties determining the role of fusion peptides in viral proteins, it has been shown that gH626–644, gB168–186, gB632–650 and gp41-FP have a similar mechanism of interaction with lipids that is consistent with their fusion peptide and/or membranotropic attributes. In particular, gB168–186 does not interact with the hydrophobic core of the membrane and translocates only slightly into the inner membrane via interaction with the lipid head groups, therefore it may work in cooperation with the second fusogenic loop in gB, and also with the other gB peptide (gB632–650) and with gH (through the gH626–644 region and the other membranotropic sequences) to complete fusion.

Recent structural studies have described a new class III of viral fusion proteins [9,70,71], and the three proteins belonging to this class, all have shown to possess a bipartite fusion peptide, which is composed of two hydrophobic loops at the tip of a four-strand β-sheet region inserted on a pleckstrin-domain. The fusion loops of gB are not buried at an oligomeric interface in the putative prefusion conformation, but cluster near the viral membrane. Moreover, any deep penetration of the peptide gB168–186, one of the fusogenic loops, inside the membrane is precluded by the presence of charged and polar residues; probably the tryptophan and phenylalanine, present in the loop, act as fingers by positioning themselves at the interface between the fatty acid chain and the head group layers of the lipids. This interaction alone is not sufficient to pull the target membrane toward the viral one but may perturbate the outer leaflet of the target bilayer facilitating the other membranotropic domains of gB and gH. All the data available point to the fact that gB alone is not sufficient for viral entry, in fact all herpesviruses also require gH and gL. The domain corresponding to gB632–650 plays a fundamental role in the fusion process. Thus, the peptide gB632–650 is particularly interesting because it presents a high inhibitory activity, a high fusion activity and a high and stable penetration inside the membrane bilayer. This peptide is located in domain IV of the protein which comprises two discontinuous segments, residues 111–116 and 573–660, linked by a disulfide bond, and contains the epitopes recognised by neutralising antibodies. The fusion process of HSV is very complicated and we are gaining information on the two main proteins involved in the process, with the aim to describe the mechanism by which gB and gH cooperate to perform fusion. Our results provide some new elements in the understanding of HSV fusion but still more work is necessary.

References

[1] L. Lins, M. Decaffmeyer, A. Thomas, R. Brasseur, Relationships between the orientation and the structural properties of peptides and their membrane interactions, Biochim. Biophys. Acta 1778 (2008) 1537–1544.
[2] J.A. Killian, T.K.M. Nyholm, Peptides in lipid bilayers: the power of simple models, Curr. Opin. Struct. Biol. 16 (2006) 473–479.
[3] S.H. White, W.C. Wimley, Hydrophobic interactions of peptides with membrane interfaces, Biochim. Biophys. Acta 1376 (1998) 339–352.
[4] S. Martens, H.T. McMahon, Mechanisms of membrane fusion: disparate players and common principles, Nat. Rev., Mol. Cell Biol. 9 (2008) 543–556.
[5] W. Weissenhorn, A. Hinz, Y. Gaudin, Virus membrane fusion, FEBS Lett. 581 (2007) 2150–2155.
[6] F.A. Rey, Molecular gymnastics at the herpesvirus surface, EMBO Rep. 7 (2006) 1000–1005.
[7] A. Farnsworth, T.W. Wisner, M. Webb, R. Roller, G. Cohen, R. Eisenberg, D.C. Johnson, Herpes simplex virus glycoproteins gB and gH function in fusion between the virion envelope and the outer nuclear membrane, Proc. Natl. Acad. Sci. U. S. A. 104 (2007) 10187–10192.
[8] J.M. White, S.E. Delos, M. Brecher, K. Schornberg, Structures and mechanisms of viral membrane fusion proteins: multiple variations on a common theme, Crit. Rev. Biochem. Mol. Biol. 43 (2008) 189–219.
[9] E.E. Heldwein, H. Lou, F.C. Bender, G.H. Cohen, R.J. Eisenberg, S.C. Harrison, Crystal structure of glycoprotein B from herpes simplex virus 1, Science 313 (2006) 217–220.
[10] R.P. Subramanian, R.J. Geraghty, Herpes simplex virus type 1 mediates fusion through a hemifusion intermediate by sequential activity of glycoproteins D, H, L, and B, Proc. Natl. Acad. Sci. U. S. A. 104 (2007) 2903–2908.
[11] S. Galdiero, A. Falanga, M. Vitiello, H. Browne, C. Pedone, M. Galdiero, Fusogenic domains in herpes simplex virus type 1 glycoprotein H, J. Biol. Chem. 280 (2005) 28632–28643.
[12] S. Galdiero, A. Falanga, M. Vitiello, M. D'Isanto, C. Collins, V. Orrei, H. Browne, C. Pedone, M. Galdiero, Evidence for a role of the membrane-proximal Region of Herpes Simplex Virus Type 1 Glycoprotein H in membrane fusion and virus inhibition, Chembiochem 8 (2007) 885–895.

[13] S. Galdiero, A. Falanga, M. Vitiello, M. D'Isanto, M. Cantisani, A. Kampanaraki, E. Benedetti, H. Browne, M. Galdiero, Peptides containing membrane-interacting motifs inhibit herpes simplex virus type 1 infectivity, Peptides 29 (2008) 1461–1471.
[14] S. Galdiero, A. Falanga, M. Vitiello, L. Raiola, R. Fattorusso, H. Browne, C. Pedone, C. Isernia, M. Galdiero, Analysis of a membrane interacting region of herpes simplex virus type1 glycoprotein H, J. Biol. Chem. 283 (2008) 29993–30009.
[15] S. Galdiero, M. Vitiello, M. D'Isanto, A. Falanga, M. Cantisani, H. Browne, C. Pedone, M. Galdiero, The identification and characterisation of fusogenic domains in herpesvirus glycoprotein B molecules, ChemBioChem 9 (2008) 758–767.
[16] A. Thomas, R. Brasseur, Tilted peptides: the history, Curr. Protein. Pept. Sci. 7 (2006) 523–527.
[17] S.E. Blondelle, K. Lohner, M. Aguilar, Lipid-induced conformation and lipid-binding properties of cytolytic and antimicrobial peptides: determination and biological specificity, Biochim. Biophys. Acta 1462 (1999) 89–108.
[18] B. Bechinger, Biophysical investigations of membrane perturbations by polypeptides using solid-state NMR spectroscopy, Mol. Membr. Biol. 17 (2000) 135–142.
[19] Y. Shai, Mechanism of the binding, insertion and destabilization of phopsholipid bilayer membranes by alpha-helical antimicrobial and cell non-selective membrane-lytic peptides, Biochim. Biophys. Acta 1462 (1999) 55–70.
[20] B. Bechinger, The structure, dynamics and orientation of antimicrobial peptides in membranes by multidimensional solid-state NMR spectroscopy, Biochim. Biophys. Acta 1462 (1999) 157–182.
[21] M.A. Cooper, Optical biosensors in drug discovery, Nat. Rev. Drug. Discov. 1 (2002) 515–528.
[22] H. Mozsolits, W.G. Thomas, M.I. Aguilar, Surface plasmon resonance spectroscopy in the study of membrane-mediated cell signalling, J. Pept. Sci. 9 (2003) 77–89.
[23] M. Besenicar, P. Macek, J.H. Lakey, G. Anderluh, Surface plasmon resonance in protein–membrane interactions, Chem. Phys. Lipids 141 (2006) 169–178.
[24] S. Heyse, T. Stora, E. Schmid, J.H. Lakey, H. Vogel, Emerging techniques for investigating molecular interactions at lipid membranes, Biochim. Biophys. Acta 1376 (1998) 319–338.
[25] H. Mozsolits, H.J. Wirth, J. Werkmeister, M.I. Aguilar, Analysis of antimicrobial peptide interactions with hybrid bilayer membrane systems using surface plasmon resonance, Biochim. Biophys. Acta 1512 (2001) 64–76.
[26] W. Wang, D.K. Smith, K. Moulding, H.M. Chen, The dependence of membrane permeability by the antibacterial peptide cecropin B and its analogues, CB-1 and CB-3, on liposomes of different composition, J. Biol. Chem. 273 (1998) 27438–27448.
[27] H. Mozsolits, M.I. Aguilar, Surface plasmon resonance spectroscopy: an emerging tool for the study of peptide–membrane interactions, Biopolymers 66 (2002) 3–18.
[28] N. Papo, Y. Shai, Exploring peptide membrane interaction using surface plasmon resonance: differentiation between pore formation versus membrane disruption by lytic peptides, Biochemistry 42 (2003) 458–466.
[29] A.S. Ladokhin, S.H. White, Detergent-like permeabilization of anionic lipid vesicles by melittin, Biochim. Biophys. Acta 1514 (2001) 253–260.
[30] D. Marsh, L.I. Horvath, Structure, dynamics and composition of the lipid–protein interface. Perspectives from spinlabelling, Biochim. Biophys. Acta 1376 (1998) 267–296.
[31] D. Marsh, T. Pali, The protein–lipid interface: perspectives from magnetic resonance and crystal structures, Biochim. Biophys. Acta 1666 (2004) 118–141.
[32] L.M. Gordon, C.C. Curtain, Y.C. Zhong, A. Kirkpatrick, P.W. Mobley, A.J. Waring, The amino-terminal peptide of HIV-1 glycoprotein 41 interacts with human erythrocyte membranes: peptide conformation, orientation and aggregation, Biochim. Biophys. Acta 1139 (1992) 257–274.
[33] C. Curtain, F. Separovic, K. Nielsen, D. Craik, Y. Zhong, A. Kirkpatrick, The interactions of the N-terminal fusogenic peptide of HIV-1 gp41 with neutral phospholipids, Eur. Biophys. J. 28 (1999) 427–436.
[34] M.J. Hope, M.B. Bally, G. Webb, P.R. Cullis, Production of large unilamellar vesicles by a rapid extrusion procedure. Characterization of size distribution, trapped volume and ability to maintain a membrane potential, Biochim. Biophys. Acta, Biomembr. 812 (1985) 55–65.
[35] E. Gazit, W.J. Lee, P.T. Brey, Y. Shai, Mode of action of the antibacterial cecropin B2: a spectrofluorometric study, Biochemistry 33 (1994) 10681–10692.
[36] D.K. Struck, D. Hoekstra, R.E. Pagano, Use of resonance energy transfer to monitor membrane fusion, Biochemistry 20 (1981) 4093–4099.
[37] E. Kalb, S. Frey, L.K. Tamm, Formation of supported planar bilayers by fusion of vesicles to supported phopsholipid monolayers, Biochim. Biophys. Acta 1103 (1992) 307–316.
[38] T.A. Morton, D.G. Myszka, I.M. Chaiken, Interpreting complex binding kinetics from optical biosensors: a comparison of linear analysis, the integrated rate equation and numerical integration, Anal. Biochem. 227 (1995) 176–185.
[39] E.J. Bolen, P.W. Holloway, Quenching of tryptophan fluorescence by brominated phospholipids, Biochemistry 29 (1990) 9638–9643.
[40] A.I. De Kroon, M.W. Soekarjo, J. De Gier, B. De Kruijff, The role of charge and hydrophobicity in peptide–lipid interaction: a comparative study based on tryptophan fluorescence measurements combined with the use of aqueous and hydrophobic quenchers, Biochemistry 29 (1990) 8229–8240.
[41] G. D'Errico, A.M. D'Ursi, D. Marsh, Interaction of a peptide derived from glycoprotein gp36 of Feline Immunodeficiency Virus and its lipoylated analogue with phospholipid membranes, Biochemistry 47 (2008) 5317–5327.
[42] R. Akkarawongsa, N.E. Pocaro, G. Case, A.W. Kolb, C.R. Brandt, Multiple peptides homologous to herpes simplex virus type 1 glycoprotein B inhibit viral infection, Antimicrob. Agents Chemother. 53 (2009) 987–996.
[43] E. Habermann, J. Jentsch, Sequence analysis of melittin from tryptic and peptic degradation products, Hoppe-Seyler Z. Physiol. Chem. 348 (1967) 37–50.
[44] M. Rafalski, J. Lear, W. DeGrado, Phospholipid interactions of synthetic peptides representing the N-terminus of HIV gp41, Biochemistry 29 (1990) 7917–7922.
[45] N. Papo, Y. Shai, Effect of drastic sequence alteration and D-amino acid incorporation on the membrane binding behavior of lytic peptides, Biochemistry 43 (2004) 6393–6403.
[46] N. Papo, Y. Shai, New lytic peptides based on the D,L-amphipathic helix motif preferentially kill tumor cells compared to normal cells, Biochemistry 42 (2003) 9346–9354.
[47] M.A. Amon, M. Ali, V. Bender, K. Hall, M.I. Aguilar, J. Aldrich-Wright, N. Manolis, Kinetic and conformational properties of a novel T-cell antigen receptor transmembrane peptide in model membranes, J. Pept. Sci. 14 (2008) 714–724.
[48] T.H. Lee, H. Mozsolits, M.I. Aguilar, Measurements of the affinity of melittin for zwitterionic and anionic membranes using immobilized lipid biosensors, J. Pept. Res. 58 (2001) 464–476.
[49] A. Niemz, D.A. Tirrell, Self-association and membrane-binding behaviour of melittin containing trifluoroleucine, J. Am. Chem. Soc. 123 (2001) 7407–7413.
[50] G. D'Errico, G. Vitiello, A.M. D'Ursi, D. Marsh, Interaction of short modified peptides deriving from glycoprotein gp36 of feline immunodeficiency virus with phospholipid membranes, Eur. Biophys. J. 38 (2009) 873–882.
[51] R. Spadaccini, G. D'Errico, V. D'Alessio, E. Notomista, A. Bianchi, M. Merola, D. Picone, Structural characterization of the transmembrane proximal region of the hepatitis C virus E1 glycoprotein, Biochim. Biophys. Acta (2009). Published on the web doi:10.1016/j.bbamem.2009.10.018.
[52] M.B. Sankaram, D. Marsh, Protein–lipid interactions with peripheral membrane proteins, in: A. Watts (Ed.), New Comprehensive Biochemistry: Protein–Lipid Interactions, Elsevier, Amsterdam, 1993, pp. 127–162, 25.
[53] D. Marsh, Protein modulation of lipids and vice versa in membranes, Biochim. Biophys. Acta 1778 (2008) 1545–1575.
[54] M. Ramakrishnan, P.H. Jensen, D. Marsh, α-synuclein association with phosphatidylglycerol probed by lipid spin labels, Biochemistry 42 (2003) 12919–12926.
[55] M.J. Swamy, D. Marsh, Spin-label electron paramagnetic resonance studies on the interaction of avidin with dimyristoyl-phosphatidylglycerol membranes, Biochim. Biophys. Acta 1513 (2001) 122–130.
[56] J.H. Davis, J.J. Clair, J. Juhasz, Phase equilibria in DOPC/DPPC-d62/cholesterol mixtures, Biophys. J. 96 (2009) 521–539.
[57] W. Hubbell, H.M. McConnell, Molecular motion in spin-labelled phospholipids and membranes, J. Am. Chem. Soc. 93 (1971) 314–326.
[58] L.M. Gordon, R.D. Sauerheber, Studies on spin-labelled egg lecithin dispersions, Biochim. Biophys. Acta 466 (1977) 34–43.
[59] L.M. Gordon, C.C. Curtain, Electron spin resonance analysis of model and biological membranes, in: R.C. Aloia, C.C. Curtain, L.M. Gordon (Eds.), Advances in Membrane Fluidity 1: Methods for Studying Membrane Fluidity, Alan R. Liss, New York, 1988, pp. 25–89.
[60] M.J. Swamy, D. Marsh, Spin-label electron spin resonance studies on the dynamics of the different phases of N-biotinylphosphatidylethanolamines, Biochemistry 33 (1994) 11656–11663.
[61] A. Lange, D. Marsh, K.H. Wassmer, P. Meier, G. Kothe, Electron spin resonance study of phospholipid membranes employing a comprehensive line-shape model, Biochemistry 24 (1985) 4383–4392.
[62] M. Moser, D. Marsh, P. Meier, K.H. Wassmer, G. Kothe, Chain configuration and flexibility gradient in phospholipid membranes. Comparison between spin-label electron spin resonance and deuteron nuclear magnetic resonance, and identification of new conformations, Biophys. J. 55 (1989) 111–123.
[63] Y.V.S. Rama Krishna, D. Marsh, Spin label ESR and 31P-NMR studies of the cubic and inverted hexagonal phases of dimyristoylphosphatidylcholine/myristic acid (1:2, mol/mol) mixtures, Biochim. Biophys. Acta 1024 (1990) 89–94.
[64] J.H. Kleinschmidt, J.E. Mahaney, D.D. Thomas, D. Marsh, Interaction of bee venom melittin with zwitterionic and negatively charged phospholipid bilayers: a spin-label electron spin resonance study, Biophys. J. 72 (1997) 767–778.
[65] T. Gianni, P.L. Martelli, R. Casadio, G. Campadelli-Fiume, The ectodomain of herpes simplex virus glycoprotein H contains a membrane α-helix with attributes of an internal fusion peptide, positionally conserved in the *Herpesviridae* family, J. Virol. 79 (2005) 2931–2940.
[66] Y. Tu, J. Kim, A fusogenic segment of glycoprotein H from her simplex virus enhances transfection efficiency of cationic liposomes, J. Gene Med. 10 (2008) 646–654.
[67] W.F. DeGrado, J.D. Lear, Conformationally constrained alpha-helical peptide models for protein ion channels, Biopolymers 29 (1990) 205–213.
[68] R.A. Parente, L. Nadasdi, N.K. Subbarao, F.C. Szoka, Association of a pH-sensitive peptide with membrane vesicles: role of amino acid sequence, Biochemistry 29 (1990) 8713–8719.
[69] J.D. Lear, W.F. DeGrado, Membrane binding and conformational properties of peptides representing the NH2 terminus of influenza HA-2, J. Biol. Chem. 262 (1987) 6500–6505.
[70] S. Roche, S. Bressanelli, F.A. Rey, Y. Gaudin, Crystal structure of the low-pH form of the vesicular stomatitis virus glycoprotein G, Science 313 (2006) 187–191.
[71] S. Roche, F.A. Rey, Y. Gaudin, S. Bressanelli, Structure of the prefusion form of the vesicular stomatitis virus glycoprotein G, Science 315 (2007) 843–848.